

1 **Heterogeneous genetic invasions of three insecticide resistance mutations in Indo-Pacific**
2 **populations of *Aedes aegypti* (L.)**

3 **Running title: Resistance by invasion in Indo-Pacific *Ae. aegypti***

4 Nancy M. Endersby-Harshman^{1*}[✉], Thomas L. Schmidt^{1*}, Jessica Chung¹, Anthony van Rooyen²,
5 Andrew R. Weeks^{1,2}, Ary A. Hoffmann¹

6 [✉]corresponding author (nancye@unimelb.edu.au)

7

8 ¹Pest and Environmental Adaptation Research Group, School of BioSciences, Bio21 Institute, 30
9 Flemington Rd, Parkville, The University of Melbourne, Victoria 3010, Australia

10 ²cesar Pty Ltd, 293 Royal Parade, Parkville Victoria 3052, Australia

11

12 *Equal first authors

13

14 **Abstract**

15 Nations throughout the Indo-Pacific region use pyrethroid insecticides to control *Aedes aegypti*, the
16 mosquito vector of dengue, often without knowledge of pyrethroid resistance status of the pest or
17 origin of resistance. Two mutations (V1016G + F1534C) in the sodium channel gene (*Vssc*) of *Ae.*
18 *aegypti* modify ion channel function and cause target-site resistance to pyrethroid insecticides, with
19 a third mutation (S989P) having a potential additive effect. Of 27 possible genotypes involving these
20 mutations, some allelic combinations are never seen while others predominate. Here, five allelic
21 combinations common in *Ae. aegypti* from the Indo-Pacific region are described and their
22 geographical distributions investigated using genome-wide SNP markers. We tested the hypothesis
23 that resistance allele combinations evolved *de novo* in populations, versus the alternative that

24 dispersal of *Ae. aegypti* between populations facilitated genetic invasions of allele combinations. We
25 used latent factor mixed-models to detect SNPs throughout the genome that showed structuring in
26 line with resistance allele combinations and compared variation at SNPs within the *Vssc* gene with
27 genome-wide variation. Mixed-models detected an array of SNPs linked to resistance allele
28 combinations, all located within or in close proximity to the *Vssc* gene. Variation at SNPs within the
29 *Vssc* gene was structured by resistance profile, while genome-wide SNPs were structured by
30 population. These results demonstrate that alleles near to resistance mutations have been
31 transferred between populations via linked selection. This indicates that genetic invasions have
32 contributed to the widespread occurrence of *Vssc* allele combinations in *Ae. aegypti* in the Indo-
33 Pacific region, pointing to undocumented mosquito invasions between countries.

34

35 Key words: insecticide resistance, voltage sensitive sodium channel (*Vssc*), single nucleotide
36 polymorphism (SNP), genetic invasion, linked selection, *Aedes aegypti*

37 Introduction

38 Once an invertebrate pest species has invaded a new area, the ability to control the new incursion
39 will depend on whether incursive populations are resistant to chemical pesticides available to control
40 them. This in turn will depend on whether the incursive populations carry pesticide resistance alleles,
41 which can arise through *in situ* evolution of resistance alleles and/or through the introduction of
42 resistance alleles from other established populations. Both processes can be important in pest and
43 disease vector control: examples of local evolution of resistance include pyrethroid resistance in the
44 earth mite *Halotydeus destructor* (Yang et al., 2020) and organophosphate resistance in the whitefly
45 *Bemisia tabaci*, while the long distance introduction of resistance genes is typified by pyrethroid
46 resistance in the mosquito *Culex pipiens* (Chevillon, Raymond, Guillemaud, Lenormand, & Pasteur,
47 1999); the contribution of both these factors in invading populations is highlighted by pesticide
48 resistance in the spider mite *Tetranychus urticae* (Shi et al., 2019) and the moth *Spodoptera*
49 *frugiperda* (Nagoshi et al., 2017).

50

51 Target-site or knockdown resistance (*kdr*) due to mutations in the sodium channel gene is one of the
52 main mechanisms that compromises control of the dengue vector mosquito, *Aedes aegypti*, with
53 pyrethroid insecticides (Smith, Kasai, & Scott, 2016). These *kdr* mutations have been detected widely
54 in pest insects, following the first discovery of the L1014F mutation in the housefly, *Musca domestica*
55 (Williamson, Denholm, Bell, & Devonshire, 1993), which conferred resistance to DDT. The term '*kdr*'
56 now covers a range of mutations in different locations in the voltage-sensitive sodium channel (*Vssc*),
57 with some being found across insect taxa and others being taxon-specific. To aid comparison of
58 mutation sites between taxa, the numbering of codons is usually kept consistent with the codon
59 numbers of the homologous region of the sodium channel gene of the housefly. Although multiple
60 mutations (synonymous and non-synonymous) have been identified in the sodium channel of *Ae.*

61 *aegypti*, only those non-synonymous mutations found in four positions (codons 1534, 1016, 1011
62 and 410) have been shown, in electrophysiological assays, to influence the function of the channel so
63 that the toxic action of pyrethroid insecticides is diminished (Du et al., 2013; Haddi et al., 2017)
64 (Figure 1).

65

66 Sodium channel mutations at codons 1016 and 1534 have been known for many years in *Ae. aegypti*
67 and occur within the pyrethroid receptor sites in Domains II (S6) and III (S6) of the protein molecule
68 (Du et al., 2013). These two mutations, V1016G and F1534C, are found in *Ae. aegypti* in the Indo-
69 Pacific region (Figure 1). A third mutation, S989P, which is often in perfect linkage with V1016G, is
70 not known to reduce the sensitivity of the sodium channel based on results of Du et al. (2013), but
71 appears to confer some additive pyrethroid resistance in the homozygous state in combination with
72 1016G in *Ae. aegypti* from Yogyakarta, Indonesia (Wuliandari et al., 2015). S989P is also found in *Ae.*
73 *aegypti* in the Indo-Pacific region. An additional mutation (D1794Y), which appears to have a similar
74 effect to S989P when found in conjunction with V1016G, is known from *Ae. aegypti* in Taiwan
75 (Chang, Huang, Chang, Wu, & Dai, 2012; Chang et al., 2009; Lin, Tsen, Tien, & Luo, 2013), and has not
76 been shown to alter the sensitivity of the sodium channel to pyrethroids in electrophysiological
77 assays (Du et al., 2013). A T1520I mutation found in *Ae. aegypti* from India is a third mutation which
78 enhances resistance rather than affecting sodium channel sensitivity by itself and has been shown to
79 increase resistance to Type I pyrethroids caused by F1534C (Chen et al., 2019).

80

81 Target-site resistance to pyrethroids is an autosomal, incompletely recessive trait controlled by a
82 single gene (Chang et al., 2012) which has important implications for the resistance status of the
83 heterozygote. Chang et al. (2012) expected the heterozygote at each site to show a level of tolerance
84 to pyrethroid insecticides which is not much higher than that of wildtype (susceptible) individuals

85 and this is the case for S989P+V1016G or F1534C in crossing experiments (Plernsub, Saingamsook,
86 Yanola, Lumjuan, Tippawangkosol, Sukontason, et al., 2016). However, Plernsub et al. (2016) found
87 some enhancement of resistance in the triple heterozygote (S989P/V1016G/F1534C) which showed
88 resistance intermediate between a 1534C homozygous mutant strain and a 989P/1016G homozygous
89 mutant strain in Thailand. Ishak et al. (2015) demonstrated a similar effect in the absence of S989P in
90 *Ae. aegypti* in Malaysia and concluded that V1016G and F1534C heterozygotes occurring in the same
91 individual have an additive effect on deltamethrin resistance of the mosquito.

92

93 Crosses performed by Plernsub et al. (2016) between a 1016GG/989PP and a 1534CC strain revealed
94 that combinations of alleles are co-inherited. A haplotype donated by one parent maintains strong
95 linkage patterns between the combination of the mutation sites. This linkage limits genotypes found
96 in offspring of crosses and in the population in general. Several studies have noted that mutant
97 homozygote 1016G is often found in conjunction with a wildtype homozygote at F1534 and *vice*
98 *versa* (Ishak et al., 2015; Kawada et al., 2014; Stenhouse et al., 2013). Synthesis of data from these
99 studies and our own observations suggest that certain haplotypes of the three mutation sites
100 predominate in a population and there is little evidence of crossing over to disrupt the phase
101 patterns found.

102

103 Management of *Ae. aegypti* as a vector of dengue and other arboviruses requires knowledge of its
104 insecticide resistance status and the likelihood of this status changing over time (Moyes et al., 2017;
105 Plernsub, Saingamsook, Yanola, Lumjuan, Tippawangkosol, Walton, et al., 2016). Mosquito
106 populations may become resistant to insecticides by local selection on new mutations or after the
107 incursion of resistant genotypes into a new region which we refer to here as a “genetic invasion”.
108 Local selection pressures from insecticides are expected to vary due to different frequencies of

109 application, rates and proportions of Type I and II pyrethroids applied, and in some cases, will select
110 for specific genotypes, as was observed in *Ae. aegypti* from Yucatan State, Mexico (Saavedra-
111 Rodriguez et al., 2015).

112

113 In the absence of strong local selection, resistance alleles are unlikely to increase in frequency in a
114 population because their selective advantage will not be realised and they may carry a fitness cost
115 (Brito et al., 2013). *Vssc* resistance alleles have not been detected in *Ae. aegypti* in northern Australia
116 (Endersby-Harshman et al., 2017) suggesting that they are either not present or occur at very low
117 frequency. If the latter case is correct, then the absence of local selection has prevented resistance
118 alleles from increasing to a detectable frequency in this location. Resistance generated through local
119 selection in one location may spread to others as mosquitoes disperse, resulting in the same
120 resistance mutations occurring in unrelated populations.

121

122 Broad-scale geographic variation in the incidence of *Vssc* mutations occurs in *Ae. aegypti*; for
123 example, in Southeast Asia the V1016G mutation is abundant, and in South America the V1016I
124 mutation occurs at the same site; V1016G is clearly causative of pyrethroid resistance while V1016I
125 alone has no effect on sodium channel sensitivity to pyrethroids, but has been shown to increase
126 resistance to both Type I and II pyrethroids in conjunction with the F1534C mutation (Chen et al.,
127 2019). At a local geographic scale, the occurrence and frequency of the 1016, 1534 and 989
128 mutations can also vary (Leong et al., 2019; C.-X. Li et al., 2015; Wuliandari et al., 2015; Yanola et al.,
129 2011). However, it is not clear if this variation reflects movement patterns of mosquitoes (genetic
130 invasion) or ongoing mutation and selection. Evidence of resistance mutations spreading as
131 mosquitoes move has been found in Ghana where mutation F1534C appeared, as a first record in

132 Africa, associated with an intron phylogeny from Southeast Asia and South America (Kawada et al.,
133 2016) (intron between exon 20 and 21 in the *Vssc* gene).

134

135 To resolve how broad-scale resistance patterns are produced, the distribution of resistance alleles
136 can be compared to patterns of genetic differentiation in high resolution single nucleotide
137 polymorphism (SNP) markers (Yang et al., 2020). As the recently developed genome assembly *Ae*g5
138 (Matthews et al., 2018) provides a precise genomic location for almost every SNP in *Ae. aegypti*, this
139 methodology can be refined to compare patterns of genetic differentiation in SNPs close to the *Vssc*
140 gene with those of more distant SNPs. Genomic approaches using SNP markers have been effective
141 at identifying differentiation in *Ae. aegypti* across a range of scales (J. E. Brown et al., 2014; Gloria-
142 Soria et al., 2018; Jasper, Schmidt, Ahmad, Sinkins, & Hoffmann, 2019; Rašić, Filipović, Weeks, &
143 Hoffmann, 2014; Schmidt, Filipovic, Hoffmann, & Rasic, 2018; Schmidt et al., 2019; Sherpa et al.,
144 2017). The clear differentiation among *Ae. aegypti* populations (Rašić et al., 2014) provides a suitable
145 background against which to compare differentiation at and around the *Vssc* gene region.

146

147 Here we report on the distribution of resistance alleles in *Ae. aegypti* from the Indo-Pacific region.
148 We focus on those *Vssc* mutations found in *Ae. aegypti* from the Indo-Pacific region that have been
149 shown in electrophysiological assays to reduce the sensitivity of the mosquito's sodium channel to
150 pyrethroid insecticides (Du et al., 2013) as well as one mutation which has no effect on channel
151 sensitivity, but may enhance resistance in association with one of the other mutations (Wuliandari et
152 al., 2015). Our study aims to (1) determine the geographical distribution of *Vssc* mutations at codons
153 989, 1016 and 1534 in *Ae. aegypti* from throughout the region; (2) compare genetic structure at sites
154 near the *Vssc* gene with sites far from the *Vssc* gene; and (3) infer the possible processes leading to
155 the *Vssc* distribution patterns found in mosquitoes throughout the Indo-Pacific.

156 **Methods**

157 *Insect collection*

158 Samples of *Ae. aegypti* were collected from the field from 43 locations covering 11 countries in the
159 Indo-Pacific region from April 2015 to February 2018 (Supplementary Table S1). Mosquitoes were
160 collected as adults or larvae from water containers and, in the case of larvae, were reared to late
161 instar stages or adults before being confirmed as *Ae. aegypti*, preserved and stored in either >70%
162 ethanol or RNAlater® (AMBION, Inc., Austin, Texas, USA).

163

164 *DNA extraction*

165 DNA was extracted from adult mosquitoes or late instar larvae using the DNeasy® Blood and Tissue
166 kit (QIAGEN Sciences, Maryland, USA) according to the instructions of the manufacturer. Two final
167 elutions of DNA were made with the first being used for construction of genomic libraries (see
168 below) and the second being used for screening of *Vssc* mutations after being diluted 1:10 with
169 water.

170

171 *Screening of Vssc mutations*

172 395 samples of *Ae. aegypti* from 11 countries were screened for *Vssc* mutations (Supplementary
173 Table S1). The amino acid positions relating to the mutation sites in this study are labelled as S989P,
174 V1016G and F1534C (Figure 1) according to the sequence of the most abundant splice variant of the
175 house fly, *Musca domestica*, *Vssc* (GenBank accession nos. AAB47604 and AAB47605) (Kasai et al.,
176 2014). These mutation sites are equivalent to those in other studies labelled as S996P, V1023G and
177 F1565C based on the *Vssc* homologue in *Ae. aegypti*, the AaNav protein (GenBank accession no.
178 EU399181) (Du et al., 2013). Custom TaqMan® SNP Genotyping Assays (Life Technologies, California,

179 USA) were developed for each of the three target site mutations (Table 1) based on sequence
180 information from Wuliandari et al. (2015).
181
182 Probes for the wildtype allele in each assay were labelled with Applied Biosystems™ VIC® reporter
183 dye in conjunction with a Minor Groove Binder (MGB) and a non-fluorescent quencher (NFQ). Probes
184 for the mutant allele were labelled with Applied Biosystems™ FAM™ reporter dye, MGB and NFQ.
185 Three replicates of each TaqMan® assay were run on a LightCycler® II 480 (Roche, Basel, Switzerland)
186 real time PCR machine in a 384-well format. The PCR Master Mix contained 40x TaqMan® assay as
187 described above (0.174 µL), 2x KAPA Fast PCR Probe Force qPCR Master Mix (KAPABIOSYSTEMS,
188 Cape Town, South Africa) (3.5 µL), ddH₂O and genomic DNA as prepared above (2 µL). Conditions for
189 the PCR run were pre-incubation of 3 min at 98°C (ramp rate 4.8°C/ s) followed by 40 cycles of
190 amplification at 95°C for 10 s (2.5°C/ s ramp rate) and 60°C for 20 s (2.5°C/ s ramp rate) (Acquisition
191 mode: single) with a final cooling step of 37°C for 1 min (2.5°C/ s ramp rate). Endpoint genotyping
192 was conducted using the Roche LightCycler® 480 Software Version 1.5.1.62.

193

194 *Testing for genetic invasions*

195 Tests for genetic invasion were conducted on a single nucleotide polymorphisms (SNP) dataset
196 comprising 80 of the *Ae. aegypti* screened for pyrethroid resistance. We investigated mosquitoes
197 from ten countries, with eight individuals from each country included in the dataset. We considered
198 individuals from the same country to be from the same population. For some populations, more than
199 eight individuals were available for inclusion; in these cases, we first selected individuals for inclusion
200 to preserve maximum variation in *Vssc* genotypes in that population (Figure 2), then selected them in
201 order of having the least missing data. Removing excess individuals ensured that genetic
202 differentiation measurements would not be biased by uneven population sample sizes. For large,

203 genome-wide SNP datasets, five genotypes per population can be sufficient for estimating genetic
204 differentiation (Willing, Dreyer, & van Oosterhout, 2012). We omitted Vietnam from these analyses
205 due to accidental loss of samples, and we also omitted populations lacking resistance mutations.
206 Supplementary Table S2 gives details of the 80 *Ae. aegypti* used to test for genetic invasions. These
207 include some individuals previously sequenced by Schmidt et al. (2019), that have been aligned to
208 the AaegL5 genome assembly (Matthews et al., 2018) used in this study.

209

210 The 80 *Ae. aegypti* were genotyped for genome-wide SNPs using the double-digest RAD sequencing
211 (ddRADseq) methodology of Rašić et al. (2014) and the bioinformatics pipeline Stacks v2.0 (Catchen,
212 Hohenlohe, Bassham, Amores, & Cresko, 2013). Reads were aligned to the AaegL5 genome assembly
213 (Matthews et al., 2018) using Bowtie2 (Langmead & Salzberg, 2012). The dataset was processed in
214 Stacks and VCFtools (Danecek et al., 2011) with the following filters: SNPs must be biallelic, be
215 present in 75% of mosquitoes in each population, have a minor allele count of ≥ 2 (following Linck
216 and Battey (2019)), have less than 5% missing data, have read depth of between 3 and 45 (following
217 (H. Li, 2014)), and have a known location on one of the three autosomes. The dataset was pre-
218 filtered to ensure no putative first-order relatives were included (all Loiselle's $k < 0.1875$; (Loiselle,
219 Sork, Nason, & Graham, 1995)). All library construction and filtering steps are detailed in the
220 Supplementary Information S1.

221

222 We assigned mosquitoes with the A, C, D, and G genotypes to a resistance profile group "Profile GTC"
223 (one or two copies of haplotype H1; Figure 2), assigned mosquitoes with the B, C, E, and H genotypes
224 to a second group "Profile TGT" (one or two copies of haplotype H2; Figure 2), assigned mosquitoes
225 with the D, E, and F genotypes to a fourth group "Profile TTT" (one or two copies of haplotype H3;
226 Figure 2), and assigned mosquitoes with the G and H genotypes to a third group "Profile GTT" (one or

227 two copies of haplotype H4; Figure 2). Note the nomenclature refers to the mutations in order of
228 degree of resistance conferred from highest to lowest, i.e. 1016/1534/989. Mosquitoes with the C, G,
229 and H genotypes each had two of the above profiles.

230

231 To look for indications that resistance alleles have spread via genetic invasion, we investigated
232 patterns of differentiation across the genomes of the 80 individuals. These analyses were motivated
233 by the expectation that, if resistance alleles had been spread by genetic invasion, we would see
234 different patterns of differentiation in SNPs around the *Vssc* gene than at other parts of the genome.
235 Among populations in which a given resistance profile has become established via genetic invasion of
236 a single *de novo* mutation, non-wildtype individuals with identical *Vssc* resistance profiles will have
237 attained these profiles from the same invasive ancestors, and thus these individuals will have alleles
238 that are identical by descent via this invasion. This shared identity by descent should be strongest
239 among alleles at SNPs within and proximate to the *Vssc* gene region (chromosome 3; positions
240 315,926,360 – 316,405,638), and, specifically, to the point mutation conferring resistance for that
241 profile. Considering the low recombination rate of *Ae. aegypti* (Bennett et al., 2005; S. E. Brown,
242 Severson, Smith, & Knudson, 2001), these patterns of linkage may remain even if gene flow ceased
243 many generations ago or involved only a small number of invasive migrants.

244

245 Accordingly, if a given resistance profile had reached its present distribution in the Indo-Pacific region
246 through genetic invasion from a single source population, we would expect to observe similar
247 patterns of variation at SNPs within and proximate to the *Vssc* gene region for individuals with that
248 resistance profile, even when they are from different populations. We would expect variation at
249 other SNPs to be structured by population, as typically observed in *Ae. aegypti* (Rašić et al., 2014;
250 Schmidt et al., 2019). In cases where a population has been recently genetically invaded, there may

251 be very little differentiation in SNPs near the *Vssc* gene among individuals with that resistance
252 profile. Overall, we would expect broad genetic similarity at the *Vssc* gene among all individuals
253 sharing a resistance profile spread via genetic invasion, as alleles near the point mutation actively
254 conferring resistance will be identical by descent. Clearly, analyses should not consider variation at
255 the resistance point mutations themselves, which would confuse any comparison of identity by state
256 and identity by descent. As ddRADseq targets only ~1% of the genome, we considered it unlikely that
257 any of the three resistance point mutations would be sequenced, and we checked to ensure that
258 none of them were.

259

260 For a population in which resistance evolved independently, we would also expect to see broad
261 similarities in genetic structure near the *Vssc* gene among individuals in that population sharing that
262 resistance profile. However, while these individuals would have the same resistance mutation
263 identical by state with individuals in other populations, the alleles near the *Vssc* gene would have no
264 identity by descent across populations. Thus, if no genetic invasions have taken place, individuals
265 with the same resistance profile would show structuring in SNPs near the *Vssc* gene along the same
266 lines as SNPs elsewhere in the genome; that is, structuring by population of origin and not by
267 resistance profile.

268

269 We performed two analyses to test for genetic invasions, both using the R package “LEA” (Frichot &
270 François, 2015). For the first analysis, we used sparse nonnegative matrix factorization (function
271 *snmf*) to investigate genome-wide patterns of genetic structure and determine an optimal number of
272 clusters (K) in which to partition the 80 *Ae. aegypti* genotypes. We then used the optimum K to
273 condition a latent factor mixed model (function *lfmm*) (Frichot, Schoville, Bouchard, & François,
274 2013), which scanned the genome for SNPs that were structured according to a set of environmental

275 variables. For these variables, we used the two resistance profiles: GTC and TGT. We ignored Profile
276 TTT for these analyses; although the susceptible, wild-type profile could serve as an interesting “null”
277 against which to compare the other profiles, almost all of the individuals of Profile TTT were
278 heterozygotes with haplotype H2 (Figure 2), thus preventing any unbiased comparison. Also, as
279 Profile GTT was only found in a single population (Taiwan), it was not appropriate for inclusion in
280 these analyses.

281

282 We ran *snmf* using 50 repetitions to determine the value of K from 1 to 10 with minimum cross-
283 entropy, which was considered the best estimate of the number of ancestral populations. We ran
284 *lfrmm* with 25 repetitions, using 10,000 iterations and 5,000 burn-in for each. The two resistance
285 profiles were each treated as distinct variables and fit separately. In each case, z-scores were
286 recalibrated using the genomic inflation factor (Frichot & François, 2015).

287

288 For the second analysis of genetic invasion, we used the function *pca* to perform two principal
289 components analyses (PCAs) on the 80 *Ae. aegypti*. The first PCA used only the SNPs that were
290 located within the *Vssc* gene region. The second PCA used SNPs that were found anywhere outside
291 the *Vssc* region. In the absence of genetic invasion, we would anticipate that both PCAs would
292 partition the genetic variance roughly equivalently, along population lines. In the case of genetic
293 invasion, we would expect the genetic variance of the *Vssc* SNPs to be structured by resistance
294 profile and that of the non-*Vssc* SNPs by population.

295

296 **Results**

297 *Vssc mutations*

298 Variation was identified in the *Vssc* alleles and genotype combinations of *Ae. aegypti* throughout the
299 Indo-Pacific region. Eight of the possible 27 combinations of genotypes of the three sodium channel
300 mutation sites were identified in the samples of *Ae. aegypti* and five of these were present in high
301 numbers (Table 2). Mutation sites 1016G and 989P were perfectly linked within our sample with
302 respect to genetic state (except in a small number of individuals from Taiwan) and were in negative
303 linkage disequilibrium with site 1534C. If we consider each possible state, namely wildtype
304 homozygote, mutant homozygote and heterozygote, only three putative haplotypes are required to
305 construct each of the observed combinations (excluding those from Taiwan) (Figure 2a). One
306 additional haplotype is required to construct the two extra genotypes from Taiwan (Figure 2b).

307

308 Patterns of *Vssc* mutations were varied across the geographic dataset. From one to five mutation
309 combinations (genotypes) were found at each geographic location with the most combinations (five)
310 being identified from the remote Republic of Kiribati and from Taiwan (Table 2). Mosquitoes from
311 Bali, Indonesia and the Republic of Vanuatu showed only one genotype pattern (homozygous mutant
312 for 1016G and 989P, but wildtype for F1534 – designated as genotype A). Mosquitoes from Vietnam,
313 New Caledonia and Fiji only showed mutations at the 1534 site (homozygous and heterozygous,
314 genotypes B and E) and the sample also contained some completely wildtype individuals (genotype
315 F). *Aedes aegypti* from Singapore, Thailand and Malaysia showed three main genotype combinations,
316 namely A, B and C (C = heterozygous at each of the three sites) (Figure 3).

317

318 *Testing for genetic invasions*

319 After filtering, we retained 50,569 genome-wide SNPs for genetic analyses, from an unfiltered set of
320 93,925 SNPs. Eighteen of these SNPs were located within the *Vssc* gene. Four of these SNPs were
321 located within a *Vssc* exon region, of which three were in the 3' untranslated region and one was in
322 the coding region. None of the SNPs corresponded to any of the three point mutations conferring
323 resistance. Mean depth across the filtered SNPs was 22.24 (s.d. 6.33) and mean missingness in
324 individuals was 1.82% (s.d. 1.23%).

325

326 Using the entire set of 50,569 SNPs, sparse nonnegative matrix factorization in LEA found $K = 4$ to be
327 the optimal choice for K (Supplementary Figure S1). Latent factor mixed-models treating Profiles GTC
328 and TGT as environmental factors found a set of SNPs strongly associated with each profile (Figure 4).
329 These SNPs were all clustered around the *Vssc* gene and had $-\log_{10}(P)$ of up to 57, while elsewhere on
330 the genome no SNP had $-\log_{10}(P) > 15$. For Profile GTC, there were 26 SNPs of $-\log_{10}(P) > 15$, all of
331 which were found in a region 4,661,744 bp long (chromosome 3; positions 313,105,794 –
332 317,767,538) surrounding and containing the *Vssc* gene (chromosome 3; positions 315,926,360 –
333 316,405,638), with eight of these SNPs found within the *Vssc* gene. For Profile TGT, there were 23
334 SNPs of $-\log_{10}(P) > 15$, which were found in a similar region 12,468,872 bp long (chromosome 3;
335 positions 305,090,719– 317,559,591) containing the *Vssc* gene. Of these 23 SNPs, eight were located
336 within the *Vssc* gene, which were the same eight SNPs detected as outliers in the latent factor mixed-
337 model for Profile GTC. Supplementary Figure S2 shows latent factor mixed-model results across a
338 narrow band of chromosome 3 (positions 300,000,000 – 330,000,000).

339

340 PCA on the 18 SNPs within the *Vssc* gene region indicated that variation at these SNPs was much
341 more clearly structured by resistance profile than by population (Figure 5a, c, e). When symbology of
342 the PCA was used to indicate individuals of Profile GTC and those not of GTC (Figure 5a), Profile GTC

343 individuals clustered to the top and to the left of most non-GTC individuals. Homozygous GTC
344 individuals (dark blue squares) clustered more tightly and more distinctly than heterozygotes (light
345 blue circles and triangles). A single non-GTC individual from Taiwan (white square) clustered with the
346 22 GTC homozygotes. Non-GTC individuals with a single copy of the haplotype H4 (green circles)
347 clustered similarly to GTC individuals with a single copy of haplotype H1 (light blue circles and
348 triangles), indicating a potential shared evolutionary origin of these haplotypes. This was also
349 indicated by the single individual with a copy of each of the H1 and H4 haplotypes (light blue circle),
350 which clustered with GTC homozygotes.

351

352 When symbology of the PCA was used to indicate individuals of Profile TGT and those not of TGT
353 (Figure 5c), most Profile TGT individuals clustered to the top and to the right of most non-TGT
354 individuals. As with Profile GTC, homozygotes (red squares) clustered more distinctly than
355 heterozygotes (orange circles and triangles). Exceptions were the single Taiwanese homozygote that
356 clustered with GTC homozygotes (white squares), and a Malaysian homozygote that clustered with
357 TGT/wildtype heterozygotes (orange upside-down triangles) and wildtype homozygotes (white
358 upside-down triangles) from New Caledonia.

359

360 When symbology of the PCA was used to indicate individuals by population (Figure 5e), no clear
361 structuring was observed among the 18 *Vssc* SNPs. This was most apparent for populations
362 containing a range of resistance profiles, such as Kiribati, Singapore, Sri Lanka, Thailand, and Taiwan.
363 Individuals from these populations were distributed broadly across the PCA plot, indicating a lack of
364 within-population similarity at the *Vssc* gene.

365

366 PCA on the 50,551 SNPs outside the *Vssc* gene presented the opposite pattern to that of the *Vssc*
367 gene (Figure 5b, d, f). Among these SNPs, genetic variation was structured unambiguously by
368 population of origin (Figure 5f) and not by resistance profile (Figure 5b, d). The clustering of
369 populations in Figure 5f reflects the $K = 4$ estimated by sparse nonnegative matrix factorization, and
370 shows population separation similar to that observed in previous studies (Schmidt et al., 2019).
371 Clusters were: (1) New Caledonia and Vanuatu; (2) Fiji and Kiribati; (3) Taiwan; and (4) all remaining
372 South and Southeast Asian populations.

373

374 Supplementary Figure S3 shows results of additional PCAs. For these, instead of using SNPs found
375 within the *Vssc* gene and those not within the *Vssc* gene, we used SNPs with $-\log_{10}(P) > 15$ associated
376 with Profiles GTC and TGT by latent factor mixed-models (Figure 4). These showed very similar
377 results to Figure 5, wherein variation at $-\log_{10}(P)$ SNPs was structured by resistance profile
378 (Supplementary Figure S3a, b) and not by population of origin (S2c, d).

379 **Discussion**

380

381 This paper has outlined the geographical distributions of three sodium channel mutations found in
382 *Ae. aegypti* from the Indo-Pacific and has presented evidence that these mutations have attained
383 their present regional distributions via genetic invasion. This evidence relates to the genetic structure
384 of SNPs at and around the *Vssc* gene, which showed that mosquitoes from different populations, but
385 with the same resistance profiles, had similar patterns of variation in SNPs near the *Vssc* gene,
386 compared with strong differentiation for the rest of the genome. These patterns indicate that the
387 two widespread *Vssc* genotypes (mutations at codons 1016 and 1534, Profiles GTC and TGT
388 respectively) have spread throughout the region by human transportation of mosquitoes. This
389 addresses an important question about how target-site resistance arises in mosquito populations,
390 which can occur through both genetic invasion and local *de novo* mutation. Our results indicate that
391 strong linkage within the *Vssc* gene region restricts which of the 27 possible genotypes can be
392 produced, which will help inform control strategies suited to local conditions, as resistance status
393 varies greatly among these genotypes. In deriving these results, we also present a detailed
394 geographical summary of pyrethroid resistance in the Indo-Pacific, a critically important region for
395 dengue control.

396

397 The negative linkage disequilibrium between *Vssc* mutations at codons 1016 and 1534 as well as the
398 perfect linkage between mutation state at codons 1016 and 989 means that there was no possibility
399 of finding an individual mosquito homozygous for all three mutations. The triple homozygous
400 mutation (989P+1016G+1534C) has been found to enhance resistance to Type I and Type II
401 pyrethroids to a very high level in *Xenopus* oocyte experiments when created artificially in the
402 laboratory (Hirata et al., 2014). Hirata et al. (2014) caution that a single crossing over event could

403 result in an individual with the triple mutation, however, this homozygous combination of mutations
404 has been found only rarely in *Ae. aegypti* from the field (Ishak et al., 2015; Kawada et al., 2014;
405 Sayono et al., 2016) in Penang, Malaysia; Myanmar and Surakarta, Indonesia and its resistance status
406 in that context is not yet clear. Our proposal of inheritance by linked haplotypes with no
407 recombination between mutation sites 1016 and 1534 may explain why the triple mutant does not
408 often arise, even though a heterozygote 1016/1534/989 is common. It is also possible that the triple
409 mutant has a high fitness cost (Hirata et al., 2014; Plernsub, Saingamsook, Yanola, Lumjuan,
410 Tippawangkosol, Sukontason, et al., 2016). A low number of *Ae. aegypti* collected from Saudi Arabia
411 have been identified as being triple mutant heterozygotes with all three mutations on the same
412 chromosome (unlike the combination of our haplotypes H1 and H2, Fig. 2a) and these individuals
413 were susceptible to deltamethrin (Al Nazawi, Aqili, Alzahrani, McCall, & Weetman, 2017).

414

415 In the absence of recombination, the presence of only three *Vssc* haplotypes (H1, H2, H3) explains
416 why 21 of the 27 genotypes do not occur in the region (excluding Taiwan). The addition of a fourth
417 haplotype (H4) in the sample from Taiwan enables formation of the two extra genotypes (G and H,
418 Fig 2) found there. If H4 were combined with H3, another of the 27 possible genotypes could be
419 constructed, but individuals of this genotype (TG/TT/TT) were not observed. The new haplotype in
420 Taiwan (H4) may be a result of recombination, with the H1 haplotype found elsewhere in the world.
421 It may be that this haplotype was introduced to Taiwan and then recombined to produce H4.
422 Alternatively, H1 and H4 could both have evolved in Taiwan, before the H1 haplotype spread
423 elsewhere, although it is then not clear why H4 has failed to spread. The effect of the genotypes G
424 and H that we found only in Taiwan on pyrethroid resistance is not known. Genotype G has also been
425 recorded in *Ae. aegypti* in Myanmar (Kawada et al., 2014), but resistance levels of mosquitoes with
426 this genotype were not tested.

427

428 Our analyses of resistance Profiles GTC and TGT indicate that genetic invasion is likely to have played
429 a significant role in establishing the current distributions of their associated haplotypes. Our latent
430 factor mixed-models detected regions surrounding the *Vssc* gene 4,661,744 and 12,468,872 bp long
431 in which there were 26 and 23 SNPs closely associated with resistance profiles (Figure 4).

432 Investigating SNPs within the *Vssc* region using PCA also showed these were structured by resistance
433 profile rather than by population (Figure 5). As alleles at these SNP loci should not be conferring any
434 selective advantage related to resistance, we can conclude that their structuring is a result of linked
435 selection with SNPs conferring resistance. We would expect to see these SNPs structured according
436 to population if resistance mutations had arisen *de novo* in populations. Instead, we see clear
437 evidence that haplotypes H1 and H2 have genetically invaded the Indo-Pacific region. While the role
438 of human transportation in establishing geographical distributions of *Aedes* mosquitoes is already
439 well recognised (Tatem, Hay, & Rogers, 2006), these results indicate that dispersal along
440 transportation networks has also helped to establish current distributions of pyrethroid resistance
441 mutations. These results stand in contrast to a similar investigation of pyrethroid resistance in
442 Australian red-legged earth mite (*Halotydeus destructor*) populations, which showed that the present
443 distribution of resistance had been attained by multiple *de novo* mutations (Yang et al., 2020).

444

445 We propose that a series of genetic invasions have established haplotype H1 in Bali, Kiribati,
446 Malaysia, Singapore, Sri Lanka, Thailand, and Vanuatu, and have established haplotype H2 in Fiji,
447 Kiribati, Malaysia, Singapore, Sri Lanka, Thailand, and Vietnam. The consistent structuring by
448 resistance profile of *Vssc* genetic variation from these populations accords with every copy of these
449 haplotypes sharing identity by descent. However, there is no indication from our results whether
450 either haplotype originated in any of these populations or elsewhere within the Indo-Pacific region,

451 which will require further sampling. For instance, we were not able to include samples from Hawaii,
452 Tahiti, or the Philippines, three Indo-Pacific locations with interesting patterns of genetic structure
453 relative to other Indo-Pacific populations (Gloria-Soria et al., 2016).

454

455 From our results, it seems likely that Taiwan and New Caledonia have also developed local resistance
456 following the same genetic invasions, though these populations both had some resistant individuals
457 that did not cluster convincingly with others having the same resistance profile (Figure 5). In Taiwan,
458 there were two such cases: one, the clustering of Haplotype H4 along similar lines as H1 (Figure 5a),
459 and another, the clustering of a single Profile TGT homozygote with Profile GTC individuals (Figure
460 5c). The first observation is best explained by the H1 and H4 haplotypes having a shared evolutionary
461 origin, with one being the ancestral haplotype and one being derived. Determining which is ancestral
462 is beyond the scope of this study and would, at minimum, require more widespread sampling
463 throughout the Indo-Pacific region. The second observation is less easily explained, but potentially
464 relates to one or more recombination events within the *Vssc* gene introducing variation associated
465 with the H1 haplotype into the H2 haplotype in Taiwan. A more comprehensive investigation of
466 resistance in Taiwanese *Ae. aegypti* will be necessary to resolve these issues. The imperfect
467 clustering of New Caledonia and haplotype H2 (Figure 5c) appears to relate more to the rareness of
468 resistance haplotypes in New Caledonia. Only five copies of H2 were observed there, compared with
469 11 copies of the wild-type H3 haplotype, which likely prevented strong structuring by resistance
470 profile. The solitary resistant homozygote (genotype B, Figure 2) from New Caledonia did cluster
471 convincingly with other resistant homozygotes, presenting evidence for genetic invasion in this
472 population.

473

474 Populations of *Ae. aegypti* studied by others have shown evidence of selective sweeps affecting this
475 gene around codons 1534 (Ishak et al., 2015) and 1016 (Wuliandari et al., 2015). Similar evidence of
476 selection has been found in *Ae. aegypti* from South America around codon 1016 (Saavedra-Rodriguez
477 et al., 2007), but segregation of South American mosquitoes from those of the Indo-Pacific region has
478 long been recognized (Smith et al., 2016), due, in particular, to the geographic restriction of V1016I
479 to South America. Saavedra-Rodriguez et al. (2007) showed high levels of recombination between
480 codons 1011 and 1016 in *Ae. aegypti* from South America, but mutations at 1011 have are not been
481 recorded in *Ae. aegypti* from the Indo-Pacific or southeast Asia (Kawada et al., 2009; Kawada et al.,
482 2014; Smith et al., 2016). Evidence for local selection of pyrethroid resistance has been obtained in
483 *Ae. aegypti* from Mexico (Saavedra-Rodriguez et al., 2015). V1016G appears to have arisen before
484 S989P (C.-X. Li et al., 2015), as S989P is never (Kawada et al., 2014) or rarely (Wuliandari et al., 2015)
485 found alone. Our data indicate that some sites have likely reached a stable point of resistance (e.g.
486 Bali, Vanuatu) given that genotypes are fixed. However, others are in flux and we expect that the
487 resistance we have recorded may change in the future. A recent study of *Ae. aegypti* in Taiwan
488 (Biduda et al., 2019) has shown an increase over time in frequency of the 1534C mutation, indicating
489 that this population is still undergoing change.

490

491 Smith et al. (2016) summarised the findings of multiple studies on the combinations of mutations
492 that lead to pyrethroid resistance as follows: the V1016G mutation found alone confers resistance to
493 Type I (those without an α -cyano group) and Type II pyrethroids (those with an α -cyano-3-
494 phenoxybenzyl group) whereas F1534C alone confers resistance only to pyrethroids of Type I and to
495 DDT (Du, Nomura, Zhorov, & Dong, 2016a). The degree of resistance induced by V1016G alone is four
496 times that of F1534C alone when expressed in *Xenopus* oocytes (Hirata et al., 2014). S989P alone in
497 *Xenopus* oocyte trials has not been shown to confer resistance (Hirata et al., 2014). The geographic

498 haplotype distribution we have observed in *Ae. aegypti* from the Indo-Pacific suggests that mosquito
499 control in Bali and Vanuatu will be very difficult with both Type I and Type II pyrethroids. Some
500 pyrethroid efficacy is likely to have been lost to various degrees in Taiwan, Kiribati, Malaysia,
501 Singapore, Sri Lanka and Thailand. Mosquito control in Fiji, Vietnam and New Caledonia with Type I
502 pyrethroids may be compromised, but Type II pyrethroids are likely to remain effective.

503

504 The potential impacts of resistance conferred by *Vssc* mutations, however, may be modified by other
505 factors. For example, Du et al. (2016b) noted context dependent effects of combinations of *Vssc*
506 mutations likely related to genetic background of the mosquito. Smith et al. (2019) found that a
507 combination of *kdr* and CYP-mediated metabolic detoxification of insecticides confers a greater than
508 additive level of resistance to *Ae. aegypti*, so there may be a selective advantage to mosquitoes
509 having both mechanisms. In that case, the spread of *kdr* mutations that we observed may have been
510 accompanied by the spread of other resistance mechanisms.

511

512 Our approach of looking at the *Vssc* mutations in the context of genetic population structure helps
513 indicate the extent of movement of resistance alleles in *Ae. aegypti* in the Indo-Pacific and provides
514 little evidence for independent evolution of pyrethroid resistance in different populations
515 throughout the region. The results of this study likely reflect a series of genetic invasions that have
516 proceeded from the initial biological invasions of the Indo-Pacific by *Ae. aegypti* (J. E. Brown et al.,
517 2014). These invasions have introduced sets of allele combinations conferring resistance to
518 insecticides used in the region. Our results point to the importance of biosecurity controls to prevent
519 resistance alleles moving to new areas with mosquito incursions. Insecticide resistance pressures
520 within a country need to be reduced in order to prevent resistance alleles becoming fixed in
521 mosquito populations.

522 **Acknowledgements**

523 We thank our mosquito collectors – Ashley Callahan, Jason Axford, Tim Hurst, Elizabeth Valerie, Craig
524 Williams. The study was funded by the Department of Agriculture and Water Resources (DAWR),
525 Australian Government; National Health and Medical Research Council with a Programme
526 Grant/Award Numbers: 1037003, 1132412; a Fellowship to Ary A. Hoffmann, NHMRC Fellowship
527 Grant no. 1118640 and the Wellcome Trust, UK. This research was facilitated by use of the Nectar
528 Research Cloud, a collaborative Australian research platform supported by the Australian Research
529 Data Commons (ARDC) and National Collaborative Research Infrastructure Strategy (NCRIS).

530

531 **Data Accessibility Statement**

532 Resistance genotype data are available within the manuscript. The aligned .bam sequence files are
533 available through the Sequence Read Archive at NCBI Genbank, BioProject ID PRJNA608612.

534

535 **Author Contributions**

536 NMEH, TLS, AAH designed the study. NMEH, TLS, JC performed research and analysed data. AvR
537 contributed assay design. NMEH, TLS, AAH, JC and ARW wrote the paper.

538

539

References

540

- 541 Al Nazawi, A. M., Aqili, J., Alzahrani, M., McCall, P. J., & Weetman, D. (2017). Combined target site
542 (*kdr*) mutations play a primary role in highly pyrethroid resistant phenotypes of *Aedes*
543 *aegypti* from Saudi Arabia. *Parasites & Vectors*, *10*(1), 161. doi:10.1186/s13071-017-2096-6
- 544 Bennett, K. E., Flick, D., Fleming, K. H., Jochim, R., Beaty, B. J., & Black, W. C. (2005). Quantitative
545 Trait Loci that control Dengue-2 virus dissemination in the mosquito *Aedes aegypti*. *Genetics*,
546 *170*(1), 185. doi:10.1534/genetics.104.035634
- 547 Biduda, S., Lin, C.-H., Saleh, F., Konradsen, F., Hansson, H., Schiøler, K. L., & Alifrangis, M. (2019).
548 Temporal pattern of mutations in the knockdown resistance (*kdr*) gene of *Aedes aegypti*
549 mosquitoes sampled from Southern Taiwan. *The American Journal of Tropical Medicine and*
550 *Hygiene*. doi:<https://doi.org/10.4269/ajtmh.19-0289>
- 551 Brito, L. P., Linss, J. G. B., Lima-Camara, T. N., Belinato, T. A., Peixoto, A. A., Lima, J. B. P., . . . Martins,
552 A. J. (2013). Assessing the effects of *Aedes aegypti kdr* mutations on pyrethroid resistance
553 and its fitness cost. *PLoS One*, *8*(4), e60878. doi:10.1371/journal.pone.0060878
- 554 Brown, J. E., Evans, B. R., Zheng, W., Obas, V., Barrera-Martinez, L., Egizi, A., . . . Powell, J. R. (2014).
555 Human impacts have shaped historical and recent evolution in *Aedes aegypti*, the dengue
556 and yellow fever mosquito. *Evolution*, *68*(2), 514-525. doi:10.1111/evo.12281
- 557 Brown, S. E., Severson, D. W., Smith, L. A., & Knudson, D. L. (2001). Integration of the *Aedes aegypti*
558 mosquito genetic linkage and physical maps. *Genetics*, *157*(3), 1299.
- 559 Catchen, J., Hohenlohe, P. A., Bassham, S., Amores, A., & Cresko, W. A. (2013). Stacks: an analysis
560 tool set for population genomics. *Molecular Ecology*, *22*(11), 3124-3140.
561 doi:10.1111/mec.12354
- 562 Chang, C., Huang, X.-Y., Chang, P.-C., Wu, H.-H., & Dai, S.-M. (2012). Inheritance and stability of
563 sodium channel mutations associated with permethrin knockdown resistance in *Aedes*
564 *aegypti*. *Pesticide Biochemistry & Physiology*, *104*(2), 136-142.
565 doi:10.1016/j.pestbp.2012.06.003
- 566 Chang, C., Shen, W.-K., Wang, T.-T., Lin, Y.-H., Hsu, E.-L., & Dai, S.-M. (2009). A novel amino acid
567 substitution in a voltage-gated sodium channel is associated with knockdown resistance to
568 permethrin in *Aedes aegypti*. *Insect Biochemistry & Molecular Biology*, *39*(4), 272-278.
569 doi:10.1016/j.ibmb.2009.01.001
- 570 Chen, M., Du, Y., Wu, S., Nomura, Y., Zhu, G., Zhorov, B. S., & Dong, K. (2019). Molecular evidence of
571 sequential evolution of DDT- and pyrethroid-resistant sodium channel in *Aedes aegypti*. *PLoS*
572 *Negl Trop Dis*, *13*(6), e0007432. doi:10.1371/journal.pntd.0007432
- 573 Chevillon, C., Raymond, M., Guillemaud, T., Lenormand, T., & Pasteur, N. (1999). Population genetics
574 of insecticide resistance in the mosquito *Culex pipiens*. *Biological Journal of the Linnean*
575 *Society*, *68*(1-2), 147-157. doi:10.1111/j.1095-8312.1999.tb01163.x
- 576 Danecek, P., Auton, A., Abecasis, G., Albers, C. A., Banks, E., DePristo, M. A., . . . Genomes Project
577 Analysis, G. (2011). The variant call format and VCFtools. *Bioinformatics*, *27*(15), 2156-2158.
578 doi:10.1093/bioinformatics/btr330
- 579 Du, Y., Nomura, Y., Satar, G., Hu, Z., Nauen, R., He, S. Y., . . . Dong, K. (2013). Molecular evidence for
580 dual pyrethroid-receptor sites on a mosquito sodium channel. *Proceedings of the National*
581 *Academy of Sciences*, *110*(29), 11785-11790.
- 582 Du, Y., Nomura, Y., Zhorov, B. S., & Dong, K. (2016a). Evidence for dual binding sites for 1,1,1-
583 trichloro-2,2-bis(p-chlorophenyl)ethane (DDT) in insect sodium channels. *Journal of*
584 *Biological Chemistry*, *291*(9), 4638-4648.

- 585 Du, Y., Nomura, Y., Zhorov, B. S., & Dong, K. (2016b). Sodium channel mutations and pyrethroid
586 resistance in *Aedes aegypti*. *Insects*, 7(4), 1-11. doi:10.3390/insects7040060
- 587 Endersby-Harshman, N. M., Wuliandari, J. R., Harshman, L. G., Frohn, V., Johnson, B. J., Ritchie, S. A.,
588 & Hoffmann, A. A. (2017). Pyrethroid susceptibility has been maintained in the dengue
589 vector, *Aedes aegypti* (Diptera: Culicidae), in Queensland, Australia. *J Med Entomol*, 54(6),
590 1649-1658. doi:10.1093/jme/tjx145
- 591 Frichot, E., & François, O. (2015). LEA: An R package for landscape and ecological association studies.
592 *Methods in Ecology and Evolution*, 6(8), 925-929. doi:10.1111/2041-210X.12382
- 593 Frichot, E., Schoville, S. D., Bouchard, G., & François, O. (2013). Testing for associations between loci
594 and environmental gradients using latent factor mixed models. *Molecular Biology and
595 Evolution*, 30(7), 1687-1699. doi:10.1093/molbev/mst063
- 596 Gloria-Soria, A., Ayala, D., Bheecarry, A., Calderon-Arguedas, O., Chadee, D. D., Chiappero, M., . . .
597 Powell, J. R. (2016). Global genetic diversity of *Aedes aegypti*. *Molecular Ecology*, 25(21),
598 5377-5395. doi:10.1111/mec.13866
- 599 Gloria-Soria, A., Lima, A., Lovin, D. D., Cunningham, J. M., Severson, D. W., & Powell, J. R. (2018).
600 Origin of a high-latitude population of *Aedes aegypti* in Washington, DC. *Am J Trop Med Hyg*,
601 98(2), 445-452. doi:10.4269/ajtmh.17-0676
- 602 Haddi, K., Tomé, H. V. V., Du, Y., Valbon, W. R., Nomura, Y., Martins, G. F., . . . Oliveira, E. E. (2017).
603 Detection of a new pyrethroid resistance mutation (V410L) in the sodium channel of *Aedes
604 aegypti*: a potential challenge for mosquito control. *Scientific Reports*, 7, 46549.
605 doi:10.1038/srep46549
- 606 Hirata, K., Komagata, O., Itokawa, K., Yamamoto, A., Tomita, T., & Kasai, S. (2014). A single crossing-
607 over event in voltage-sensitive Na⁺ channel genes may cause critical failure of dengue
608 mosquito control by insecticides. *PLoS Negl PLoS Neglected Tropical Diseases*, 8(8), e3085.
609 doi:10.1371/journal.pntd.0003085
- 610 Ishak, I. H., Jaal, Z., Ranson, H., & Wondji, C. S. (2015). Contrasting patterns of insecticide resistance
611 and knockdown resistance (*kdr*) in the dengue vectors *Aedes aegypti* and *Aedes albopictus*
612 from Malaysia. *Parasites & Vectors*, 8(1), 1-13. doi:10.1186/s13071-015-0797-2
- 613 Jasper, M., Schmidt, T. L., Ahmad, N. W., Sinkins, S. P., & Hoffmann, A. A. (2019). A genomic approach
614 to inferring kinship reveals limited intergenerational dispersal in the yellow fever mosquito.
615 *Molecular Ecology Resources*, 0(0). doi:10.1111/1755-0998.13043
- 616 Kasai, S., Komagata, O., Itokawa, K., Shono, T., Ng, L. C., Kobayashi, M., & Tomita, T. (2014).
617 Mechanisms of pyrethroid resistance in the dengue mosquito vector, *Aedes aegypti*: target
618 site insensitivity, penetration, and metabolism. *PLoS Neglected Tropical Diseases*, 8(6),
619 e2948. doi:10.1371/journal.pntd.0002948
- 620 Kawada, H., Higa, Y., Futami, K., Muranami, Y., Kawashima, E., Osei, J. H., . . . Minakawa, N. (2016).
621 Discovery of point mutations in the Voltage-Gated Sodium Channel from African *Aedes
622 aegypti* populations: Potential phylogenetic reasons for gene introgression. *PLoS Neglected
623 Tropical Diseases*, 10(6), e0004780. doi:10.1371/journal.pntd.0004780
- 624 Kawada, H., Higa, Y., Komagata, O., Kasai, S., Tomita, T., Nguyen Thi, Y., . . . Takagi, M. (2009).
625 Widespread distribution of a newly found point mutation in Voltage-Gated Sodium Channel
626 in pyrethroid-resistant *Aedes aegypti* populations in Vietnam. *PLoS Neglected Tropical
627 Diseases*, 3(10), 1-7. doi:10.1371/journal.pntd.0000527
- 628 Kawada, H., Oo, S. Z. M., Thauang, S., Kawashima, E., Maung, Y. N. M., Thu, H. M., . . . Minakawa, N.
629 (2014). Co-occurrence of point mutations in the Voltage-Gated Sodium Channel of
630 pyrethroid-resistant *Aedes aegypti* populations in Myanmar. *PLoS Neglected Tropical
631 Diseases*, 8(7), 1-8. doi:10.1371/journal.pntd.0003032
- 632 Langmead, B., & Salzberg, S. L. (2012). Fast gapped-read alignment with Bowtie 2. *Nature methods*,
633 9(4), 357-359. doi:10.1038/nmeth.1923

- 634 Leong, C. S., Vythilingam, I., Liew, J. W. K., Wong, M. L., Wan-Yusoff, W. S., & Lau, Y. L. (2019).
635 Enzymatic and molecular characterization of insecticide resistance mechanisms in field
636 populations of *Aedes aegypti* from Selangor, Malaysia. *Parasites and Vectors*, 12(1).
637 doi:10.1186/s13071-019-3472-1
- 638 Li, C.-X., Kaufman, P. E., Xue, R.-D., Zhao, M.-H., Wang, G., Yan, T., . . . Zhao, T.-Y. (2015). Relationship
639 between insecticide resistance and *kdr* mutations in the dengue vector *Aedes aegypti* in
640 Southern China. *Parasites & Vectors*(325). doi:10.1186/s13071-015-0933-z
- 641 Li, H. (2014). Toward better understanding of artifacts in variant calling from high-coverage samples.
642 *Bioinformatics (Oxford, England)*, 30(20), 2843-2851. doi:10.1093/bioinformatics/btu356
- 643 Lin, Y.-H., Tsen, W.-L., Tien, N.-Y., & Luo, Y.-P. (2013). Biochemical and molecular analyses to
644 determine pyrethroid resistance in *Aedes aegypti*. *Pesticide Biochemistry and Physiology*,
645 107(2), 266-276. doi:<https://doi.org/10.1016/j.pestbp.2013.08.004>
- 646 Linck, E., & Battey, C. J. (2019). Minor allele frequency thresholds strongly affect population structure
647 inference with genomic data sets. *Molecular Ecology Resources*, 19(3), 639-647.
648 doi:10.1111/1755-0998.12995
- 649 Loiselle, B. A., Sork, V. L., Nason, J., & Graham, C. (1995). Spatial genetic structure of a tropical
650 understory shrub, *Psychotria officinalis* (Rubiaceae). *American Journal of Botany*, 82(11),
651 1420-1425. doi:10.1002/j.1537-2197.1995.tb12679.x
- 652 Matthews, B. J., Dudchenko, O., Kingan, S. B., Koren, S., Antoshechkin, I., Crawford, J. E., . . . VossHall,
653 L. B. (2018). Improved reference genome of *Aedes aegypti* informs arbovirus vector control.
654 *Nature*, 563(7732), 501-507. doi:10.1038/s41586-018-0692-z
- 655 Moyes, C. L., Vontas, J., Martins, A. J., Ng, L. C., Koou, S. Y., Dusfour, I., . . . Weetman, D. (2017).
656 Contemporary status of insecticide resistance in the major *Aedes* vectors of arboviruses
657 infecting humans. *PLoS Neglected Tropical Diseases*, 11(7), e0005625.
658 doi:10.1371/journal.pntd.0005625
- 659 Nagoshi, R. N., Fleischer, S., Meagher, R. L., Hay-Roe, M., Khan, A., Murúa, M. G., . . . Westbrook, J.
660 (2017). Fall armyworm migration across the Lesser Antilles and the potential for genetic
661 exchanges between North and South American populations. *PLoS One*, 12(2), e0171743.
662 doi:10.1371/journal.pone.0171743
- 663 Plernsub, S., Saingamsook, J., Yanola, J., Lumjuan, N., Tippawangkosol, P., Sukontason, K., . . .
664 Somboon, P. (2016). Additive effect of knockdown resistance mutations, S989P, V1016G and
665 F1534C, in a heterozygous genotype conferring pyrethroid resistance in *Aedes aegypti* in
666 Thailand. *Parasites & Vectors*, 9(1), 417. doi:10.1186/s13071-016-1713-0
- 667 Plernsub, S., Saingamsook, J., Yanola, J., Lumjuan, N., Tippawangkosol, P., Walton, C., & Somboon, P.
668 (2016). Temporal frequency of knockdown resistance mutations, F1534C and V1016G, in
669 *Aedes aegypti* in Chiang Mai city, Thailand and the impact of the mutations on the efficiency
670 of thermal fogging spray with pyrethroids. *Acta Tropica*, 162, 125-132.
671 doi:<http://dx.doi.org/10.1016/j.actatropica.2016.06.019>
- 672 Rašić, G., Filipović, I., Weeks, A. R., & Hoffmann, A. A. (2014). Genome-wide SNPs lead to strong
673 signals of geographic structure and relatedness patterns in the major arbovirus vector, *Aedes*
674 *aegypti*. *BMC Genomics*, 15(1), 275. doi:10.1186/1471-2164-15-275
- 675 Saavedra-Rodriguez, K., Beaty, M., Lozano-Fuentes, S., Denham, S., Garcia-Rejon, J., Reyes-Solis, G., . . .
676 Black, W. C. (2015). Local evolution of pyrethroid resistance offsets gene flow among *Aedes*
677 *aegypti* collections in Yucatan State, Mexico. *The American Journal of Tropical Medicine and*
678 *Hygiene*, 92(1), 201-209. doi:10.4269/ajtmh.14-0277
- 679 Saavedra-Rodriguez, K., Urdaneta-Marquez, L., Rajatileka, S., Moulton, M., Flores, A. E., Fernandez-
680 Salas, I., . . . Black IV, W. C. (2007). A mutation in the voltage-gated sodium channel gene
681 associated with pyrethroid resistance in Latin American *Aedes aegypti*. *Insect Molecular*
682 *Biology*, 16(6), 785-798.

- 683 Sayono, S., Hidayati, A. P. N., Fahri, S., Sumanto, D., Dharmana, E., Hadisaputro, S., . . . Syafruddin, D.
684 (2016). Distribution of Voltage-Gated Sodium Channel (Nav) alleles among the *Aedes aegypti*
685 populations in Central Java Province and its association with resistance to pyrethroid
686 insecticides. *PLoS One*, *11*(3), 1-12. doi:10.1371/journal.pone.0150577
- 687 Schmidt, T. L., Filipovic, I., Hoffmann, A. A., & Rasic, G. (2018). Fine-scale landscape genomics helps
688 explain the slow spatial spread of *Wolbachia* through the *Aedes aegypti* population in Cairns,
689 Australia. *Heredity (Edinb)*, *120*(5), 386-395. doi:10.1038/s41437-017-0039-9
- 690 Schmidt, T. L., van Rooyen, A. R., Chung, J., Endersby-Harshman, N. M., Griffin, P. C., Sly, A., . . .
691 Weeks, A. R. (2019). Tracking genetic invasions: Genome-wide single nucleotide
692 polymorphisms reveal the source of pyrethroid-resistant *Aedes aegypti* (yellow fever
693 mosquito) incursions at international ports. *Evolutionary Applications*, *12*(6), 1136-1146.
694 doi:10.1111/eva.12787
- 695 Sherpa, S., Rioux, D., Goindin, D., Fouque, F., François, O., & Després, L. (2017). At the origin of a
696 worldwide invasion: Unraveling the genetic makeup of the Caribbean bridgehead
697 populations of the dengue vector *Aedes aegypti*. *Genome Biology and Evolution*, *10*(1), 56-
698 71. doi:10.1093/gbe/evx267
- 699 Shi, P., Cao, L.-J., Gong, Y.-J., Ma, L., Song, W., Chen, J.-C., . . . Wei, S.-J. (2019). Independently evolved
700 and gene flow-accelerated pesticide resistance in two-spotted spider mites. *Ecology and*
701 *Evolution*, *9*. doi:10.1002/ece3.4916
- 702 Smith, L. B., Kasai, S., & Scott, J. G. (2016). Pyrethroid resistance in *Aedes aegypti* and *Aedes*
703 *albopictus*: Important mosquito vectors of human diseases. *Pesticide Biochemistry &*
704 *Physiology*, *133*, 1-12. doi:10.1016/j.pestbp.2016.03.005
- 705 Smith, L. B., Sears, C., Sun, H., Mertz, R. W., Kasai, S., & Scott, J. G. (2019). CYP-mediated resistance
706 and cross-resistance to pyrethroids and organophosphates in *Aedes aegypti* in the presence
707 and absence of *kdr*. *Pesticide Biochemistry and Physiology*, *160*, 119-126.
708 doi:10.1016/j.pestbp.2019.07.011
- 709 Stenhouse, S. A., Plernsub, S., Yanola, J., Lumjuan, N., Dantrakool, A., Choochote, W., & Somboon, P.
710 (2013). Detection of the V1016G mutation in the voltage-gated sodium channel gene of
711 *Aedes aegypti* (Diptera: Culicidae) by allele-specific PCR assay, and its distribution and effect
712 on deltamethrin resistance in Thailand. *Parasites & Vectors*, *6*(1), 253-253.
713 doi:10.1186/1756-3305-6-253
- 714 Tatem, A. J., Hay, S. I., & Rogers, D. J. (2006). Global traffic and disease vector dispersal. *Proceedings*
715 *of the National Academy of Sciences*, *103*(16), 6242-6247. doi:10.1073/pnas.0508391103
- 716 Williamson, M. S., Denholm, I., Bell, C. A., & Devonshire, A. L. (1993). Knockdown resistance (*kdr*) to
717 DDT and pyrethroid insecticides maps to a sodium channel gene locus in the housefly (*Musca*
718 *domestica*). *Molecular and General Genetics*, *240*(1), 17-22. doi:10.1007/BF00276878
- 719 Willing, E. M., Dreyer, C., & van Oosterhout, C. (2012). Estimates of genetic differentiation measured
720 by F(ST) do not necessarily require large sample sizes when using many SNP markers. *PLoS*
721 *One*, *7*(8), e42649. doi:10.1371/journal.pone.0042649
- 722 Wuliandari, J., Lee, S., White, V., Tantowijoyo, W., Hoffmann, A., & Endersby-Harshman, N. (2015).
723 Association between three mutations, F1565C, V1023G and S996P, in the voltage-sensitive
724 sodium channel gene and knockdown resistance in *Aedes aegypti* from Yogyakarta,
725 Indonesia. *Insects*, *6*(3), 658.
- 726 Yang, Q., Umina, P. A., Rašić, G., Bell, N., Fang, J., Lord, A., & Hoffmann, A. A. (2020). Origin of
727 resistance to pyrethroids in the redlegged earth mite (*Halotydeus destructor*) in Australia:
728 repeated local evolution and migration. *Pest Management Science*, *76*(2), 509-519.
729 doi:10.1002/ps.5538
- 730 Yanola, J., Somboon, P., Walton, C., Nachaiwieng, W., Somwang, P., & Prapanthadara, L.-a. (2011).
731 High-throughput assays for detection of the F1534C mutation in the voltage-gated sodium
732 channel gene in permethrin-resistant *Aedes aegypti* and the distribution of this mutation

733 throughout Thailand. *Tropical Medicine & International Health: TM & IH*, 16(4), 501-509.
734 doi:10.1111/j.1365-3156.2011.02725.x

735

736

737 Table 1. Custom TaqMan[®] SNP Genotyping Assays (Life Technologies, California, USA) for each of three target site mutations in the *Vssc* gene of *Aedes*

Codon	Location in <i>Vssc</i> gene	Forward primer 5' – 3'	Reverse primer 5' – 3'	Probe wildtype	Probe mutant	Amino Acid	Amplicon size bp
989	P-region which links membrane spanning segments S5 and S6 in Domain II	TTCATGATCGTGTCCGGGTATT	ACGTCACCCACAAGCATACAAT	CCCACATGGATTCGAT	CCACATGGGTTCGAT	TCC (Serine) wildtype, CCC (Proline) mutant	53
1016	First codon of exon 21 (domain II, segment 6)	CGTGCTAACCGACAAATTGTTCC	ATGAACCGAAATTGGACAAAAGCAA	AGAAAAGGTTAAGTACCTGTGCG	AAGGTTAAGTCCCTGTGCG	GTA (Valine) wildtype, GGA (Glycine) mutant	52
1534	24 th codon of exon 31 (domain III, segment 6)	TCTACATGTACCTCTACTTTGTGTTCTTCA	GATGATGACACCGATGAACAGATTC	AACGACCCGAAGATGA	ACGACCCGCAGATGA	TTC (Phenylalanine) wildtype, TGC (Cysteine) mutant	52

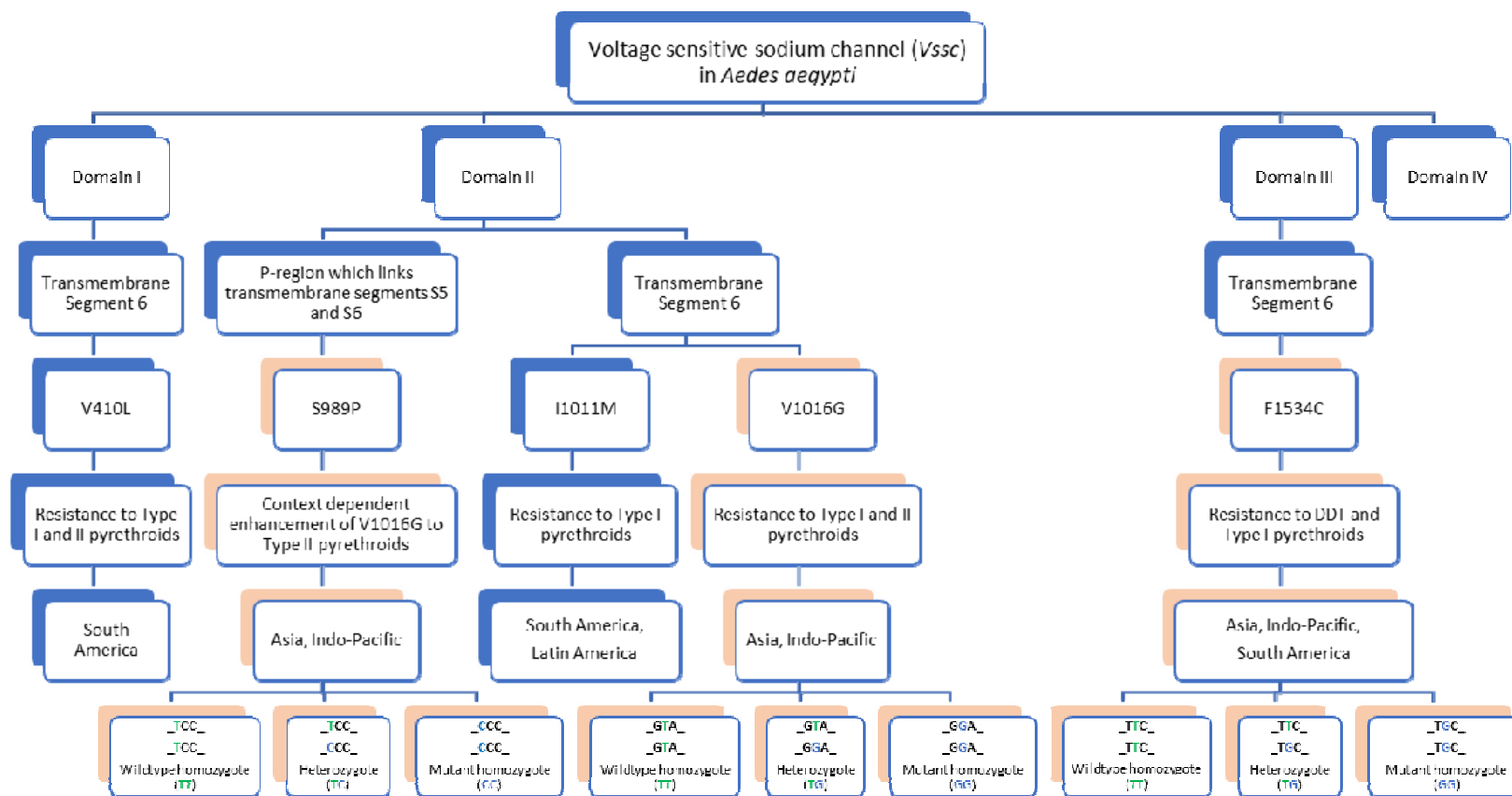
738 *aegypti* from the Indo-Pacific

739

740

741 Table 2. Frequency of *Vssc kdr* genotypes identified in *Ae. aegypti* from specific countries in the Indo-Pacific region

Genotype code:			A	B	C	D	E	F	G	H
1016/1534/989:			GGTCC	TTGGTT	TGTGTC	TGTTTC	TTTGTT	TTTTTT	GGTTC	TGTGTT
Country	n	Profile:	GTC	TGT	GTC, TGT	GTC	TGT	TTT	GTC	TGT
Taiwan	20		0.05	0.60	0.10				0.15	0.10
Sri Lanka	24			0.17		0.04	0.63	0.17		
Indonesia (Bali)	67		1.00							
Singapore	29		0.21	0.24	0.55					
Malaysia	30			0.40	0.60					
Thailand	40		0.25	0.50	0.25					
Vietnam	97			0.11			0.47	0.41		
Vanuatu	20		1.00							
New Caledonia	24			0.04			0.33	0.63		
Fiji	24			0.71			0.21	0.08		
Kiribati	20		0.10	0.45	0.25	0.05	0.15			
TOTAL	395		0.27	0.23	0.13	0.01	0.19	0.15	0.01	0.01

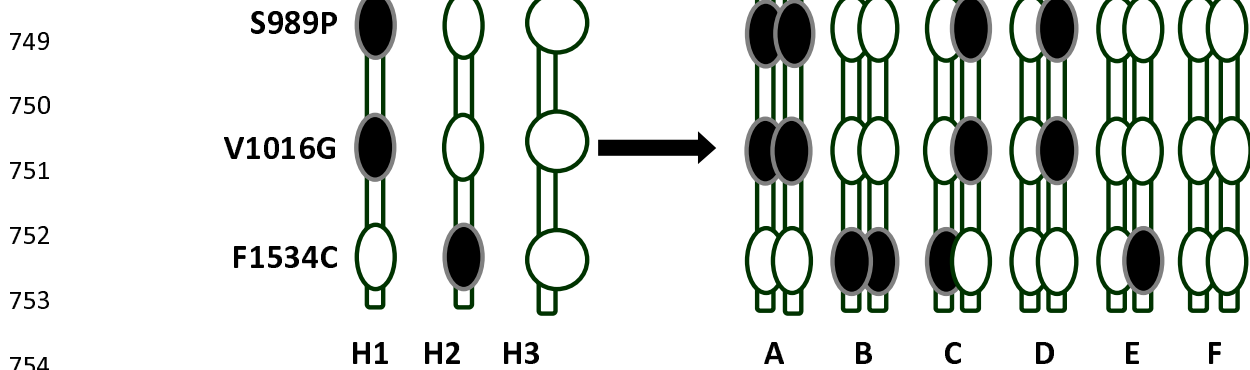


742

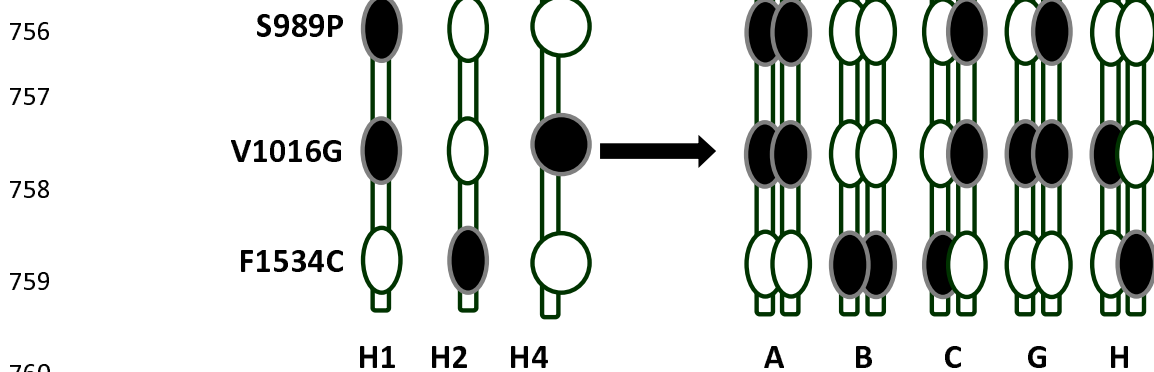
743 Figure 1. Key to *Vssc* mutations in *Aedes aegypti* that have been functionally characterised and shown to affect the *Vssc* (except for S989P). Codons
 744 are numbered according to the homologous sodium channel gene in the house fly, *Musca domestica*. Pink boxes refer to mutations screened in
 745 mosquitoes from the Indo-Pacific in this study. Information has been compiled from (Du et al., 2013; Du et al., 2016b; Haddi et al., 2017; Saavedra-
 746 Rodriguez et al., 2007; Wuliandari et al., 2015).

747

748 a.



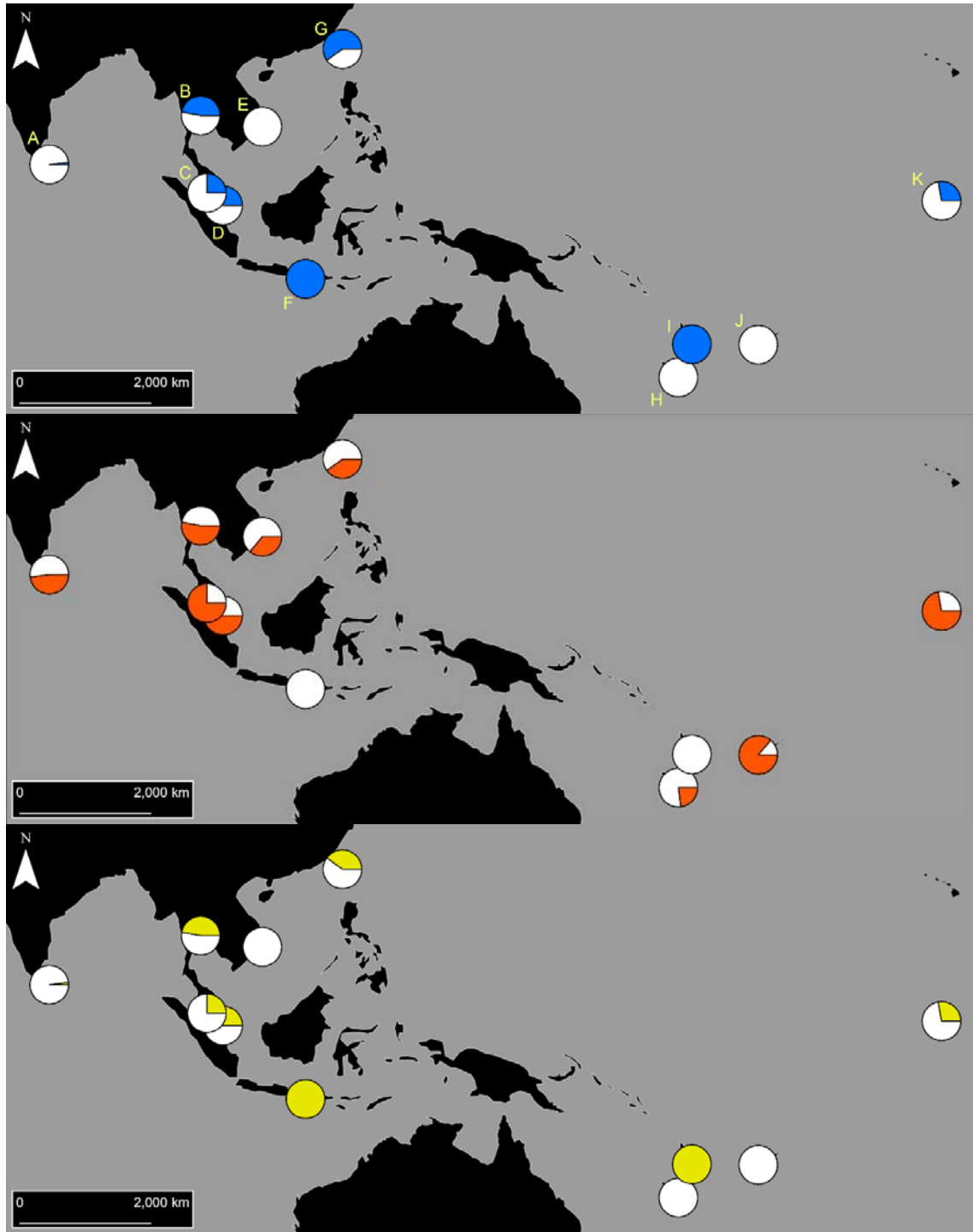
755 b.



761



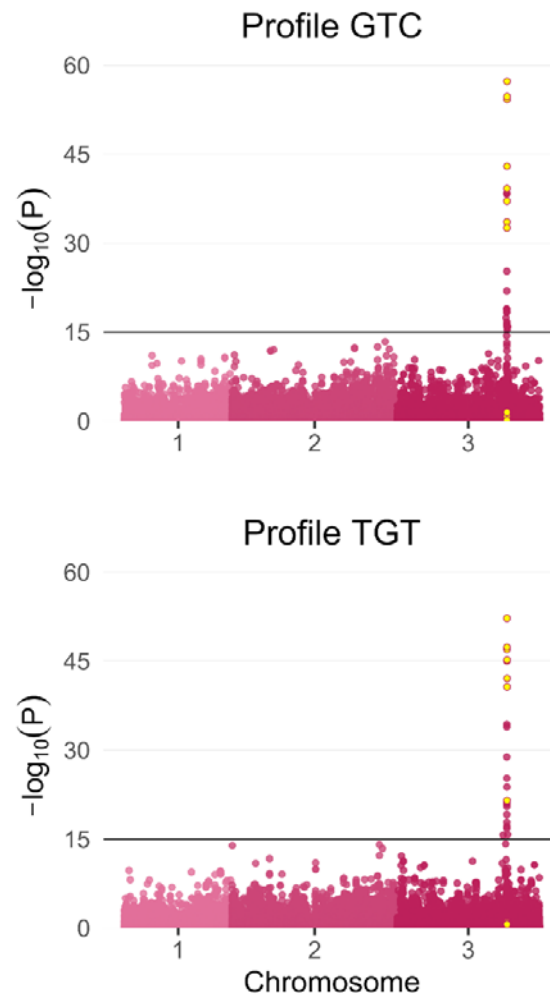
762 Figure 2 a). Putative haplotypes and phase of
 763 common mutant *Vssc kdr* genotypes of *Aedes aegypti* found in the Indo-Pacific region (excluding
 764 Taiwan sample), b) Putative haplotypes required to construct genotypes found in Taiwan sample.
 765 (Note that H1 = Profile GTC and H2 = Profile TGT).



766

767 Figure 3. Distribution of the *Vssc* mutations in Indo-Pacific *Aedes aegypti* considered in this study.
768 Coloured sectors indicate the frequency of each type of resistance mutation within each country,
769 following: Blue = 1016G, Orange = 1534C, Yellow = 989P. Populations are: (A) Sri Lanka, (B) Thailand,
770 (C) Malaysia, (D) Singapore, (E) Vietnam, (F) Bali, (G) Taiwan, (H) New Caledonia, (I) Vanuatu, (J) Fiji,
771 and (K) Kiribati.

772



773

774

775 Figure 4. Latent factor mixed-models for Profiles GTC (top) and TGT (bottom).

776 Models use $K = 4$ to condition for population structure among the 80 *Ae. aegypti*. Circles indicate

777 locations and $-\log_{10}(P)$ of SNPs. Yellow-filled circles indicate SNPs located within the *Vssc* gene

778 (chromosome 3; positions 315,926,360 – 316,405,638).

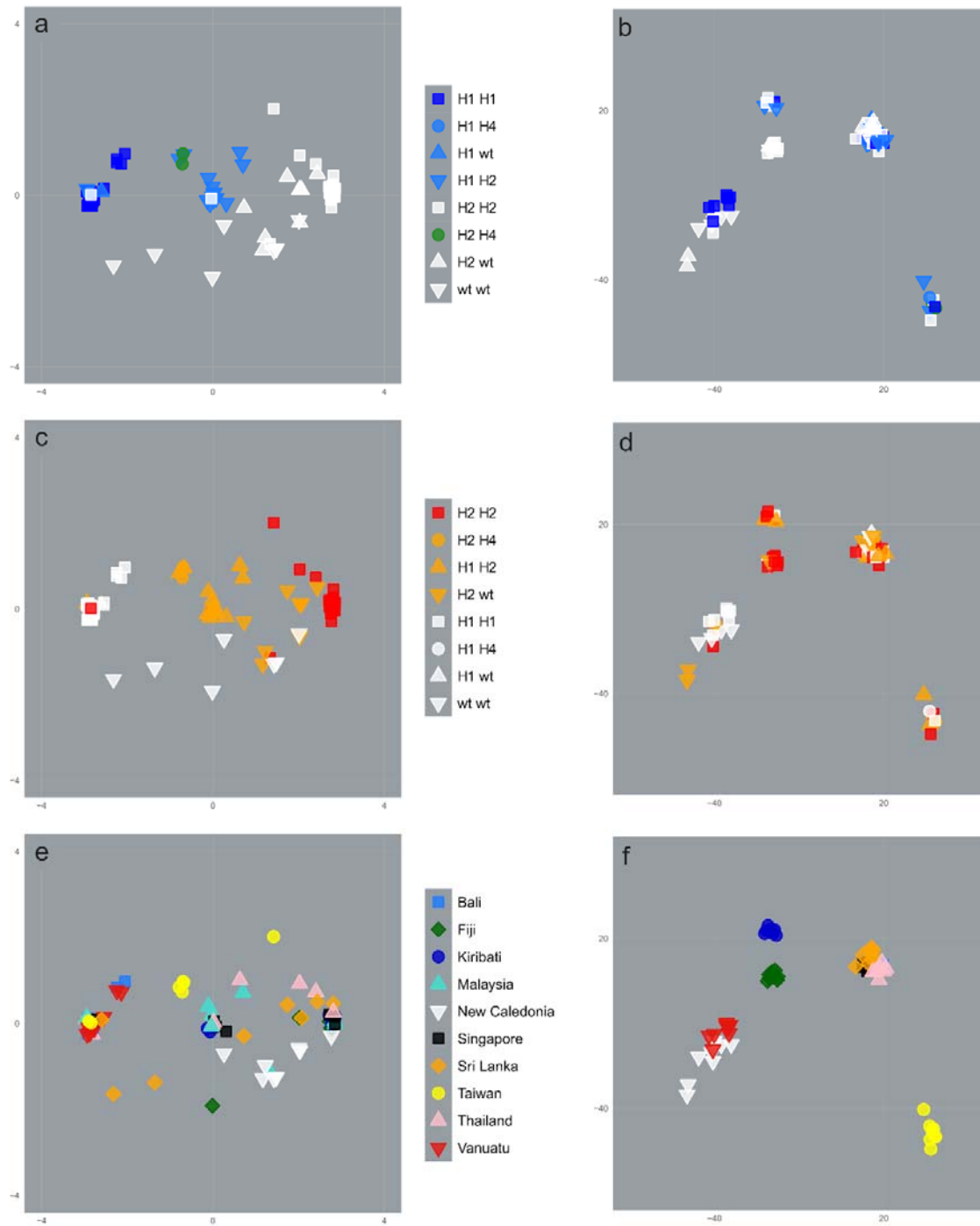


Figure 5. PCAs of 80 *Ae. aegypti* from 10 countries.

PCAs show variation at 18 SNPs within the *Vssc* gene (a, c, e) and at 50,551 SNPs outside the *Vssc* gene (b, d, f). PCAs use symbols indicating: individuals of Profile GTC and not of GTC (a, b); individuals of Profile TGT and not of TGT (c, d); and individuals by population (e, f). The green colour used in (a) and (b) reflects the uncertainty surrounding the evolutionary history of haplotype 4. For a, c, and e:

PC1 (x-axis) variation = 77.1%, PC2 (y-axis) = 5.9%. For b, d, and f: PC1 (x-axis) variation = 6.7%, PC2 (y-axis) = 4.3%.